

# Spatio-Temporal Dynamics of Free and Bound Carriers in Photovoltaic Materials

George C. Fish and Jacques-E. Moser\*

**Abstract:** Photoinduced charge separation into free carriers and subsequent charge transfer are key processes that govern the efficiencies of third generation solar cell technologies based on donor-acceptor heterojunctions. As these processes typically occur on picosecond to femtosecond timescales, it is necessary to employ ultrafast spectroscopic methods to enhance our understanding and provide vital information that can aid in furthering material design. Within the framework of the National Centre of Competence in Research “Molecular Ultrafast Science and Technology” (NCCR MUST), we have developed and utilized a suite of different ultrafast optical, infrared and terahertz techniques to study charge generation, separation, and transport in a variety of small molecule based organic and lead halide perovskite solar cells. Here, we provide an overview of the main techniques used in our laboratory and examples of recent results obtained using these experimental tools.

**Keywords:** Lead halide perovskites · Charge carrier dynamics · Organic semiconductors · Ultrafast spectroscopy



**Members of the Photochemical Dynamics Group.** From the left: Arun Paraecattil, Marine Bouduban, Juan Manuel Moreno Naranjo, George Fish, Andrés Burgos Caminal, Brener Vale, Etienne Socie, and Jacques-Edouard Moser.



**George Fish** completed his undergraduate studies in chemistry at Imperial College London where he undertook his master thesis in the group of Prof. James Durrant. He moved to Lausanne in 2018 and began his PhD in the group of Prof. Jacques-E. Moser at EPFL, where he studies ultrafast processes in organic semiconductors and perovskite solar cells.

## 1. Introduction

Photoinduced charge separation at donor-acceptor heterojunctions is a concept central to many applications including photocatalysis,<sup>[1]</sup> photovoltaics,<sup>[2]</sup> photography,<sup>[3]</sup> information storage,<sup>[4]</sup> and xerography.<sup>[5]</sup> A sound understanding of the photophysical phenomena that underpin the binding of charge carriers in excitons, polarons and charge transfer states, as well as the fate of

free charges is necessary to aid in the design and optimization of new systems of technological relevance. Furthermore, there is also interest from a fundamental scientific standpoint in the fields of physical chemistry and condensed matter physics, as the mechanisms of exciton dissociation and carrier separation dynamics are not fully established or understood.

The research carried out in the Group for Photochemical Dynamics, within the framework of NCCR MUST, focuses on investigating the mechanisms of photoinduced charge separation in third generation solar materials such as in dye-sensitized solar cells, small-molecule organic photovoltaics and hybrid organic-inorganic lead halide perovskites. Whilst diverse in their material makeup, these different technologies all generate charges via a donor-acceptor heterojunction. The general principle of such systems is as follows: firstly, photons are absorbed in an active material, generating pairs of charges of opposite signs. These charges can then undergo a charge transfer process across an interface between a donor and an acceptor material, with positive charges (holes) being present in the donor material, whilst the electrons are transported in the acceptor material. In contrast to first- (Si, GaAs) and second-generation (CIGS, CdTe) p-n junction photovoltaics where carriers of opposite signs separate in a built-in electric field, charge separation in donor-acceptor systems relies on a kinetic competition between forward and back-electron transfer steps. Ultrafast time-resolved spectroscopic techniques are necessary to probe the charge generation and separation processes, both of which play a key role in determining the overall efficiency of photovoltaic devices.

Organic materials and, in a lesser extent, perovskites are media characterized by a low permittivity. Coulomb interaction between charges of opposite signs can, therefore, be important and result in their association in bulk excitons. Charge transfer states and charge transfer excitons (CTEs) can also be formed with charge pairs being located astride the donor-acceptor heterojunction. Self-trapping of photocarriers in the form of polarons and trapping within deeper states obviously affect their mobility and transport.

Various ultrafast techniques have been employed to directly monitor photogenerated quasi-particles (excitons, CTEs, polarons, polaritons, ...) and bound carrier states. Among them, ultrafast broadband time-resolved terahertz, optical pump – IR push –

\*Correspondence: Prof. Dr J.-E. Moser, E-mail: je.moser@epfl.ch, Group for Photochemical Dynamics, Institute of Chemical Science and Engineering, École polytechnique fédérale de Lausanne, EPFL SB ISIC GR-MO, Station 6, CH-1015 Lausanne (Switzerland).

THz probe, and time-resolved electroabsorption spectroscopies have been developed and implemented in our laboratory. They have been used in tandem with other conventional techniques, such as femtosecond transient absorption and broadband fluorescence up-conversion spectroscopies, to provide insight into a variety of photophysical processes in both organic and lead halide perovskite solar cells.

## 2. Hot Carrier Mobility Dynamics in 3D Lead Halide Perovskites

Lead trihalide perovskites (LHPs) have surged over the past ten years, becoming one of the most desirable materials for optoelectronic applications. They have been used to great effect in solar cells; double heterojunction (p-i-n) photovoltaic systems based on an intrinsic LHP absorbing layer, tin or titanium dioxide as an acceptor and organic spiro-OMeTAD as the donor material have demonstrated device power conversion efficiencies of over 25%.<sup>[6]</sup> The perovskite has the general formula  $ABX_3$ , forming an octahedral crystalline structure where A is a large organic or inorganic cation (such as methylammonium,  $MA^+$ , formamidinium,  $FA^+$ , or cesium,  $Cs^+$ ), B is a divalent metal cation (such as  $Pb^{2+}$  or  $Sn^{2+}$ ) and X is a halide anion.

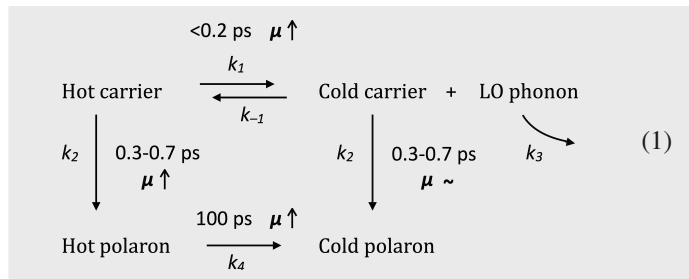
LHPs are direct-bandgap semiconductors, whose absorption threshold can be easily tuned over the entire visible wavelength domain by selecting  $X = Cl, Br, I$ , or mixtures of these halides in various proportions. The mechanisms which lead to the large photocarrier diffusion length and the high device performance of LHPs are still debated, with hot carrier cooling and polaron formation known to play an important role in the charge separation process. To examine these phenomena, an ultrabroadband time-resolved terahertz spectroscopy (TRTS) setup was used in conjunction with femtosecond transient absorption spectroscopy, allowing the monitoring of photocarrier mobility changes in real time.

TRTS is a pump-probe technique utilizing ultrashort visible pump and THz (far IR) probe pulses. In our case, the THz probe is generated using a two-color plasma technique,<sup>[7]</sup> yielding ultrabroadband THz spectra (1-25 THz). The advantage of this technique, over more conventional optical rectification in solid semiconductors, is the short THz pulse duration (200 fs vs 1 ps) it offers,<sup>[8]</sup> which is advantageous for studying the early dynamics of charge carriers. The transmitted THz beam is detected using a home-built air-biased-coherent-detection (ABCD) system.<sup>[9]</sup>

Hot carrier dynamics of LHPs with different chemical compositions were analyzed using ultrabroadband TRTS. Samples were fabricated on high density polyethylene slides to ensure full transparency to the THz pulses. By exploiting the sensitivity of THz radiation to carrier mobility, fluence and wavelength dependence measurements were used to demonstrate a competition between carrier cooling and dynamic screening, allowing us to propose a model (shown in Scheme 1) to explain the fluence dependence and the constant lifetime of the mobility rise, thus unifying the previously reported phenomena of a phonon bottleneck and polaron formation.<sup>[10]</sup>

The perovskite composition was found to predominantly impact the time constant of the dynamic screening, with  $Cs^+$  resulting in a slower process when compared to its organic counterparts, a result that can be explained by a reduction in the degrees of freedom that allow for the lattice to be polarized in the presence of charge carriers.<sup>[10]</sup>

Further developments have also been made to the TRTS setup to enable optical pump – IR push – THz probe spectroscopy (PPTPS) measurements to be conducted. This is where an infrared pulse, termed the ‘push’ pulse, irradiates the sample at a certain time delay after excitation by the pump pulse which can result in the detrapping of charge carriers as well as the splitting of charge transfer excitons (CTEs). By changing the time delay between



Scheme 1. Scheme detailing the different processes occurring in LHPs resulting in an observed rise in the carrier mobility ( $\mu$ ) as measured using TRTS. Carrier cooling and hot polaron formation induced a strong increase in the mobility within the measured time window. Longitudinal optical (LO) phonons, thought to be produced upon polaron cooling, are not observable due to being outside of the time window of the measurement. Reproduced from ref. <sup>[10]</sup>

the pump and the push pulses it is possible to determine the time evolution of these processes, whilst tuning the push wavelength can give information on the binding energy of species such as CTEs. Proof of concept experiments were carried out on mesoscopic  $TiO_2$  layers. The decrease of the THz mobility of electrons showed that about one third of charge carriers generated upon photoexcitation gets trapped with a time constant of 3 ps (Fig. 1). Application of a NIR push pulse 17 ps after the pump led to detrapping and a subsequent increase in the THz photo-conductivity measured. After detrapping, a similar number of charge carriers became trapped a second time, with both trapping processes proceeding with the same time constant.

## 3. Exciton and Carrier Dynamics in 2D Perovskites

Despite their high device efficiencies, one issue that has consistently plagued 3D perovskites is their environmental stability, in particular with respect to humidity.<sup>[11]</sup> To help minimize these issues, two-dimensional (2D) perovskites can be made, where the A cation is replaced with a larger organic cation (eg. phenethyl-ammonium, PEA) acting as a spacer thus preventing the formation of a 3D crystalline structure.<sup>[12]</sup>

These perovskites form a layered structure consisting of planes of  $PbX_6$  octahedra separated by the organic spacer. 2D perovskites can either be used on their own or be deposited atop conventional 3D perovskites, where their stability is enhanced by the outward exposition of a monolayer consisting of the hydrophobic moieties of the large cation spacers.<sup>[13]</sup> Depending on whether a monovalent or divalent spacer is used there are two different structures of 2D perovskites that can be formed.<sup>[14,15]</sup>

Despite having become a major area of interest within the field of perovskite optoelectronics, there is still uncertainty surrounding the process of hot carrier generation and cooling, exciton formation, and the potential generation of hot excitons in two-dimensional LHPs, where a strong quantum and dielectric confinement of charge carriers prevails.

To selectively probe excitons within 2D perovskites, broadband fluorescence upconversion spectroscopy (FLUPS) was used in combination with TRTS. Broadband FLUPS is a time-resolved photo-luminescence technique where the fluorescence is gated by an ultrashort laser pulse with the complete emission spectrum being measured for each time delay in a single scan pump-gate measurement, without any mechanical movement of the up-converting crystal.<sup>[16]</sup> This results in a fs resolution, which is required to build a deeper understanding of ultrafast processes occurring in perovskites.<sup>[17]</sup>

After conducting fluence dependence FLUPS and TRTS measurements exciting at 400 nm and 510 nm we were able to conclude that sequential carrier cooling and exciton formation were

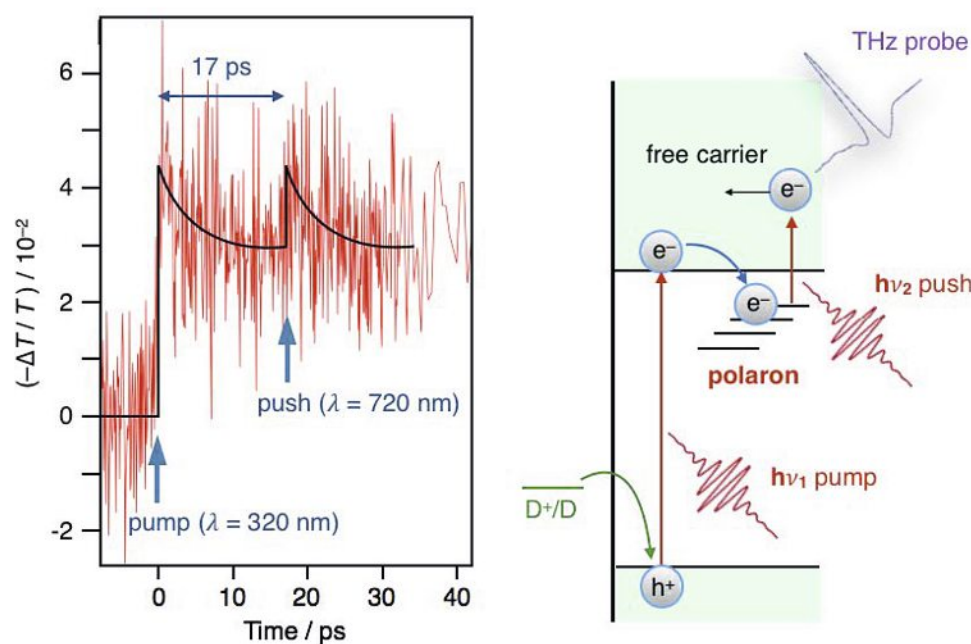
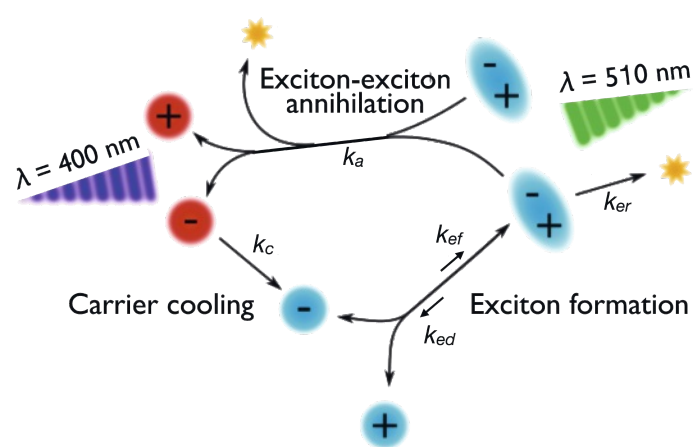


Fig. 1. THz dynamics recorded in a proof of principle PPTPS measurement of  $\text{TiO}_2$  colloidal nanoparticles. By analyzing the amplitude of the THz signal, it is possible to determine that approximately one third of the conduction band electrons are trapped following excitation, followed by detrapping upon the irradiation of a near-IR push pulse.

able to accurately describe the dynamics observed in these measurements (Scheme 2); furthermore, we were able to show that exciton-exciton interactions play a key role in the form of Auger heating and biexciton formation resulting in a longer lived population of carriers.



Scheme 2. The kinetic model which relates hot carriers (in red), cold carriers (blue) and excitons generated after photoexcitation at 400 and 510 nm. The rate constants,  $k$ , are used to describe the processes of carrier cooling ( $k_c$ ), exciton formation and dissociation ( $k_{ef}$  and  $k_{ed}$ , respectively), exciton-exciton annihilation ( $k_a$ ) and exciton recombination ( $k_{er}$ ). Reproduced from ref. [18]

The influence of the organic cation was once again studied, and whilst the impact on the steady state photophysics are minimal, it was found that the cation plays a crucial role in determining sample stability under illumination, as well as impacting upon hot carrier cooling, thus strongly affecting phonon bottleneck effects.<sup>[18]</sup>

#### 4. Carrier and Quasi-Particle Dynamics in Colloidal Perovskite Nanoplatelets

Whilst 3D perovskites still rule the roost when it comes to photovoltaics, it is also possible to confine the bulk 3D structure into materials of reduced dimensionalities such as nanoplatelets

(2D), nanorods (1D) and quantum dots (0D). This leads to new applications including photodetectors,<sup>[19]</sup> LEDs,<sup>[20]</sup> and lasing materials.<sup>[21]</sup> The quantum confinement introduced in the formation of perovskite nanocrystals results in a large exciton binding energy which leads to greatly increased photoluminescence when compared to their 3D counterparts.<sup>[22]</sup>

However, whilst the photoluminescence can be further enhanced for strongly confined regimes (defined as being at least one dimension smaller than the exciton Bohr radius), this is accompanied by an increase in the surface to volume ratio resulting in an abundance of surface defects. Understanding the photophysical processes of these trap states is vital for improving device performance.

Here, both FLUPS and fs-transient absorption spectroscopy were used in tandem to obtain a complete photophysical picture of the spectroscopic properties of strongly confined perovskite nanocrystals. A fast (3-10 ps) decay of the photoluminescence of quasi-1D  $\text{CsPbBr}_3$  perovskite nanocrystals was evidenced using FLUPS and was assigned to the reversible trapping of band-edge excitons into dark states lying close to the band edge.

Furthermore, the impact of aging on the perovskite nanocrystals was investigated (Fig. 2), where deep trap states formed because of ligand desorption from the nanocrystal surface resulted in a decrease in the photoluminescence quantum yield.<sup>[23]</sup>

Further investigations into strongly confined  $\text{CsPbBr}_3$  perovskite nanoplatelets revealed that emissive band edge states which form instantaneously upon photoexcitation relax, within the first picosecond, into confined hole states. The impact of nanoplatelet concentration was then studied and it was found that when the concentration of nanoplatelets became very high the nanoparticles overlap, thus causing a decrease in their absorption cross-section and a subsequent increase in the Stokes shift of the emission as a result of photon reabsorption.<sup>[24]</sup>

#### 5. Proof of High Efficiency Intrinsic Charge Generation in Organic Salt Semiconductors

Within the field of organic optoelectronics, devices based on small molecules are growing in their usage. Dye molecules such as cyanine, squaraine and diketopyrrolopyrrole (DPP) are of particular interest due to several advantageous properties such as the facile tuneability of their absorption spectra and high extinction coefficients, allowing them to be used to great effect in bilayer



architecture devices.<sup>[25,26]</sup> Elsewhere in the optoelectronic field, cyanine dyes have also been used in organic photodiodes to take advantage of their high absorption in the near infrared and their propensity to form J-aggregates.<sup>[27,28]</sup> Recently, pristine pentamethine cyanine dyes (Cy5) have been shown to exhibit intrinsic photogeneration of charges, despite an absence of a donor-acceptor interface.<sup>[29]</sup>

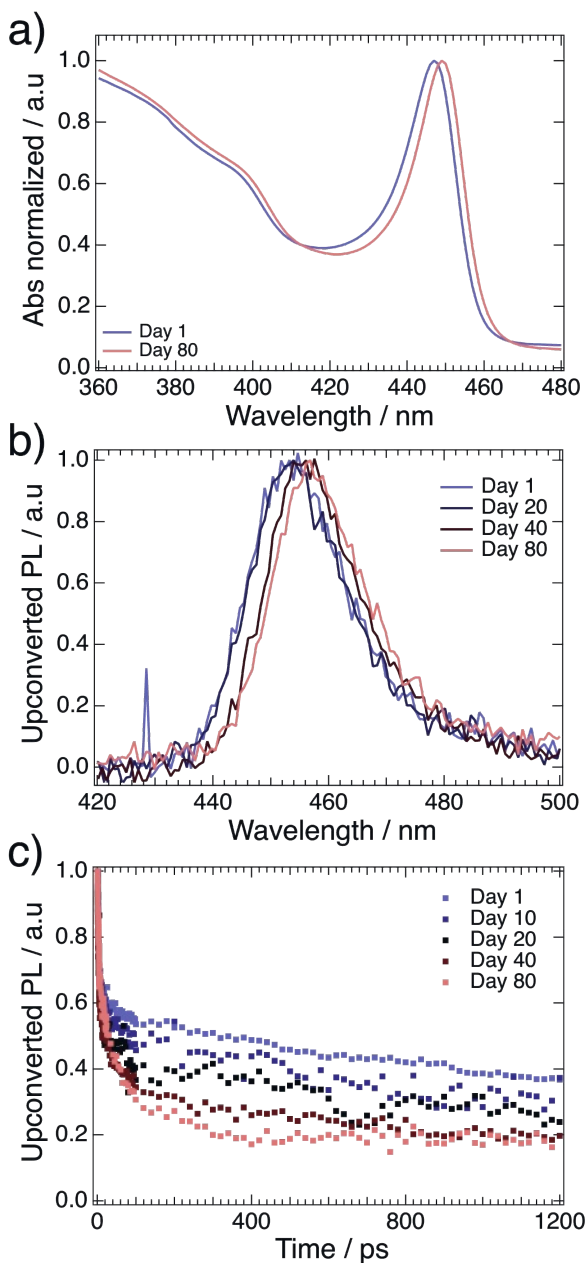


Fig. 2. a) Absorption spectra of fresh (blue) and aged (red) CsPbBr<sub>3</sub> nanoplatelets. b) Normalized emission spectra, taken at  $t = 1$  ps, for samples of different ages. c) Normalized PL decays, at  $\lambda_{em} = \lambda_{max}$  for samples of different ages. Reproduced from ref. [23].

Understanding the mechanism of this intrinsic charge generation could therefore present new material design concepts for future organic photovoltaics (OPVs) and photodiodes. Transient absorption spectroscopy was used to monitor the charge transfer processes occurring in single layer Cy5 thin films incorporating hexafluorophosphate counterions (Fig. 3).

Excitation of the thin film yielded oxidized Cy5 species, gen-

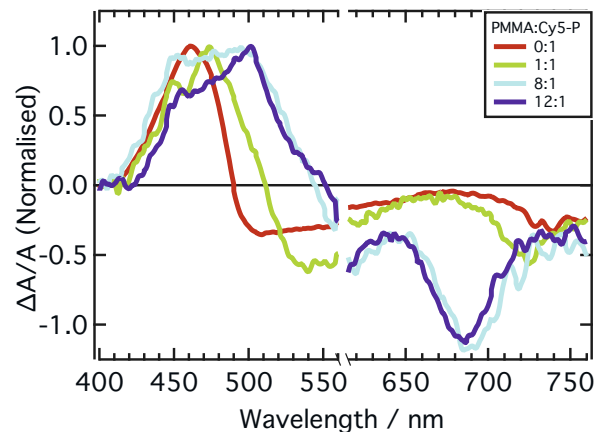


Fig. 3. Transient absorption spectra of solid thin films of PF<sub>6</sub><sup>-</sup> salts of the cyanine dye Cy5 (Cy5-P) diluted by polymethylmethacrylate polymer (PMMA) with various PMMA: Cy5-P blend ratios. Samples were excited at 580 nm. With increasing proportion of PMMA there is a decrease in H-aggregation within the sample and the positive feature, which is assigned to oxidized Cy5 chromophores, shifts from 470 nm to 500 nm. A second feature is resolved corresponding to the singlet excited state of the dye. This demonstrates the impact of H-aggregation on the charge transfer process in pristine Cy5 thin films. Adapted from ref. [30]

erated from a charge transfer process between Cy5 monomers and their H-aggregate counterparts. This symmetry breaking photo-induced charge generation process was found to proceed with a yield of up to 86 %, thus providing the first direct proof of high efficiency intrinsic charge generation in organic salt semiconductors.

Counterions have been shown to play an important role in controlling thin film properties and device efficiency in cyanine based OPVs. Therefore, we also studied the impact of counterion size on the intrinsic charge generation process. The degree of H-aggregation, which provides the driving force for the symmetry breaking charge separation, diminishes with increasing anion size, resulting in a reduced yield of charge transfer. Interestingly, however, there was little change in the carrier mobility, as the increase in interchromophore distance is compensated for by a reduction in charge trapping by H-aggregates.<sup>[30]</sup>

## 6. Dissociation of Charge Transfer States in Bilayer Organic Solar Cells

Cyanine dyes have typically been employed as donor materials in bilayer architecture organic solar cells, alongside fullerene-based acceptors. Whilst bilayer architecture device efficiencies are lower than those achieved using bulk heterojunctions, their simpler morphology allows for a clearer understanding of the charge separation processes occurring in organic solar cells.

Charge transfer (CT) states are formed in the process of charge carrier generation in organic solar cells, and their formation has been well studied. However, studies on bulk heterojunction architecture OPVs have yielded different conclusions on how these states stabilise and subsequently split into free carriers.<sup>[31-34]</sup>

By taking advantage of the simpler bilayer device morphology, the dissociation and subsequent charge separation of CT states in C<sub>60</sub>:Cy3-P bilayers was investigated in order to determine the mechanism of CT state dissociation in OPVs.

Time resolved electroabsorption spectroscopy (TREAS) was used to probe the interfacial CT states. This is a technique whereby an electric field is applied across the sample causing a shift in the absorption spectrum of a material as a result of the Stark effect.<sup>[35]</sup> Upon photoexcitation of the sample with a pump beam, charges are generated. As these charges separate from each other, the

local field between them opposes that of the applied electric field. The resulting decrease of the field experienced by the surrounding material and of the associated optical Stark shift translates to a time-resolved change of the electroabsorption spectrum. As the recorded signal depends on the distance separating charges of opposite signs, the carrier mobility and spatio-temporal information can be extracted (Fig. 4).

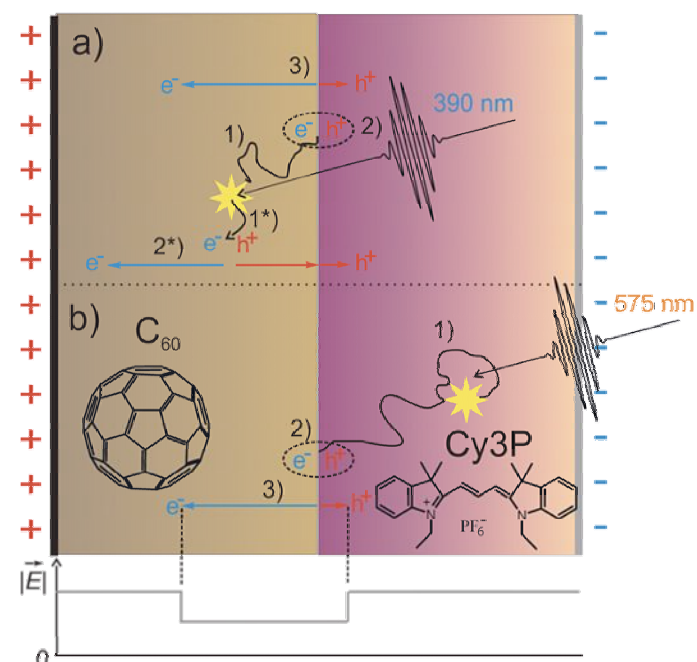


Fig. 4. Illustration of charge formation in a  $C_{60}$ :Cy3-P bilayer architecture organic solar cell. The processes that occur after excitation, with a) showing  $C_{60}$  excitation and b) Cy3-P excitation, are: (1) exciton diffusion to the D-A interface; (2) the formation and subsequent splitting of the interfacial charge transfer state; (3) the drift of free charge carriers away from the D-A interface. (1\*) and (2\*) refer to the electric field assisted generation and drift of free charge carriers in bulk  $C_{60}$ , respectively. Adapted from ref. [38].

TREAS can be used in different ways, for example to study the impact of phase morphology in polymer:fullerene blends,<sup>[36]</sup> the dynamics of photocarriers in perovskites<sup>[37]</sup> or, in this case, charge transfer states in organic bilayers. As the electroabsorption signal corresponding to Cy3-P and  $C_{60}$  appeared in different regions of the spectrum, it was possible to independently monitor the dynamics in each material using TREAS. The results indicated that electron motion was responsible for carrier separation, whilst further modelling of the electroabsorption dynamics allowed us to determine that the rate limiting process for free carrier generation is the escape of electrons from the Coulomb potential in fullerene domains. These results have important implications regarding future design of electron acceptor materials.<sup>[38]</sup>

### Acknowledgements

Financial support from the Swiss National Science Foundation, NCCR MUST, SCIE-X-NMS, and EPFL is gratefully acknowledged. The authors thank the research groups of Profs Michael Grätzel (Laboratory for Photonics and Interfaces, EPFL, Lausanne) and Frank Nüesch (Laboratory for Functional Polymers, EMPA, Dübendorf) for fruitful collaborations.

- [1] Q. Wang, K. Domen. *Chem. Rev.* **2020**, *120*, 919, <https://doi.org/10.1021/acs.chemrev.9b00201>.
- [2] J. Yan, B. R. Saunders. *RSC Adv.* **2014**, *4*, 43286, <https://doi.org/10.1039/C4RA07064J>.
- [3] I. R. Gould, J. R. Lenhard, A. A. Muentner, S. A. Godleski, S. Farid. *Pure Appl. Chem.* **2001**, *73*, 455, <https://doi.org/10.1351/pac200173030455>.
- [4] Y. Shang, Y. Wen, S. Li, S. Du, X. He, L. Cai, Y. Li, L. Yang, H. Gao, Y. Song. *J. Am. Chem. Soc.* **2007**, *129*, 11674, <https://doi.org/10.1021/ja0742226>.
- [5] J. Pan, U. Scherf, A. Schreiber, R. Bilke, D. Haarer. *Synth. Met.* **2000**, *115*, 79, [https://doi.org/10.1016/S0379-6779\(00\)00349-0](https://doi.org/10.1016/S0379-6779(00)00349-0).
- [6] J. Jeong, M. Kim, J. Seo, H. Lu, P. Ahlawat, A. Mishra, Y. Yang, M. A. Hope, F. T. Eickemeyer, M. Kim, Y. J. Yoon, I. W. Choi, B. P. Darwich, S. J. Choi, Y. Jo, J. H. Lee, B. Walker, S. M. Zakeeruddin, L. Emsley, U. Rothlisberger, A. Hagfeldt, D. S. Kim, M. Grätzel, J. Y. Kim. *Nature* **2021**, *592*, 381, <https://doi.org/10.1038/s41586-021-03406-5>.
- [7] K. Y. Kim, A. J. Taylor, J. H. Glowina, G. Rodriguez. *Nat. Photon.* **2008**, *2*, 605, <https://doi.org/10.1038/nphoton.2008.153>.
- [8] H. K. Nienhuys, V. Sundström. *Phys. Rev. B.* **2005**, *71*, 235110, <https://doi.org/10.1103/PhysRevB.71.235110>.
- [9] N. Karpowicz, J. Dai, X. Lu, Y. Chen, M. Yamaguchi, H. Zhao, X.-C. Zhang. *Appl. Phys. Lett.* **2008**, *92*, 011131, <https://doi.org/10.1063/1.2828709>.
- [10] A. Burgos-Caminal, J. M. Moreno-Naranjo, A. R. Willauer, A. A. Paracattil, A. Ajdarzadeh, J.-E. Moser. *J. Phys. Chem. C* **2021**, *125*, 98, <https://doi.org/10.1021/acs.jpcc.0c08492>.
- [11] a) G. Niu, W. Li, F. Meng, L. Wang, H. Dong, Y. Qiu. *J. Mater. Chem. A* **2014**, *2*, 705; b) J. M. Frost, K. T. Butler, F. Brivio, C. H. Hendon, M. van Schilfegaarde, A. Walsh. *Nano Lett.* **2014**, *14*, 2584, <https://doi.org/10.1021/nl500390f>.
- [12] J. Ye, H. Zheng, L. Zhu, G. Liu, X. Zhang, T. Hayat, X. Pan, S. Dai. *Sol. RRL* **2017**, *1*, 1, <https://doi.org/10.1002/solr.201700125>.
- [13] R. Garai, R. K. Gupta, M. Hossain, P. K. Iyer. *J. Mater. Chem. A* **2021**, *9*, 26069, <https://doi.org/10.1039/D1TA06901B>.
- [14] X. Gao, X. Zhang, W. Yin, H. Wang, Y. Hu, Q. Zhang, Z. Shi, V. L. Colvin, W. W. Yu, Y. Zhang. *Adv. Sci.* **2019**, *6*, 1900941, <https://doi.org/10.1002/advs.201900941>.
- [15] A. Dučinskas, G. C. Fish, M. A. Hope, L. Merten, D. Moia, A. Hinderhofer, L. C. Carbone, J.-E. Moser, F. Schreiber, J. Maier, J. V. Milič, M. Grätzel. *J. Phys. Chem. Lett.* **2021**, *12*, 10325, <https://doi.org/10.1021/acs.jpcclett.1c02937>.
- [16] M. Gerecke, G. Bierhance, M. Gutmann, N. P. Ernstring, A. Rosspeintner. *Rev. Sci. Instrum.* **2016**, *87*, 053115, <https://doi.org/10.1063/1.4948932>.
- [17] D. Tamborini, M. Buttafava, A. Ruggeri, F. Zappa. *IEEE Sens. J.* **2016**, *16*, 3827, <https://doi.org/10.1109/JSEN.2016.2535403>.
- [18] A. Burgos-Caminal, E. Socie, M. E. F. Bouduban, J.-E. Moser. *J. Phys. Chem. Lett.* **2020**, *11*, 7692, <https://doi.org/10.1021/acs.jpcclett.0c02425>.
- [19] C. H. Kang, I. Dursun, G. Liu, L. Sinatra, X. Sun, M. Kong, J. Pan, P. Maity, E.-N. Ooi, T. K. Ng, O. F. Mohammed, O. M. Bakr, B. S. Ooi. *Light: Sci. Appl.* **2019**, *8*, 94, <https://doi.org/10.1038/s41377-019-0204-4>.
- [20] R. Wang, Y. Zhang, F.-X. Yu, Y. Dong, Y.-L. Jia, X.-J. Ma, Q. Xu, Y. Deng, Z.-H. Xiong, C.-H. Gao. *J. Lumin.* **2020**, *219*, 116915, <https://doi.org/10.1016/j.jlumin.2019.116915>.
- [21] J. Xu, X. Li, J. Xiong, C. Yuan, S. Semin, T. Rasing, X.-H. Bu. *Adv. Mater.* **2020**, *32*, 1806736, <https://doi.org/10.1002/adma.201806736>.
- [22] Y. Jiang, X. Wang, A. Pan. *Adv. Mater.* **2019**, *31*, 1806671, <https://doi.org/10.1002/adma.201806671>.
- [23] E. Socie, B. R. C. Vale, A. Burgos-Caminal, J.-E. Moser. *Adv. Optical Mater.* **2021**, *9*, 2001308, <https://doi.org/10.1002/adom.202001308>.
- [24] E. Socie, B. R. C. Vale, A. T. Terpstra, M. A. Schiavon, J.-E. Moser. *J. Phys. Chem. C* **2021**, *125*, 14317, <https://doi.org/10.1021/acs.jpcc.1c01353>.
- [25] R. Hany, B. Fan, F. Araujo de Castro, J. Heier, W. Kylberg, F. Nüesch. *Prog. Photovoltaics* **2011**, *19*, 851, <https://doi.org/10.1002/pip.1049>.
- [26] E. Berner, T. Jäger, T. Lanz, F. Nüesch, J.-N. Tisserant, G. Wicht, H. Zhang, R. Hany. *Appl. Phys. Lett.* **2013**, *102*, 183903, <https://doi.org/10.1063/1.4804599>.
- [27] A. C. Véron, H. Zhang, A. Linden, F. Nüesch, J. Heier, R. Hany, T. Geiger. *Org. Lett.* **2014**, *16*, 1044, <https://doi.org/10.1021/ol4034385>.
- [28] T. P. Osedach, A. Iacchetti, R. R. Lunt, T. L. Andrew, P. R. Brown, G. M. Akselrod, V. Bulović. *Appl. Phys. Lett.* **2012**, *101*, 113303, <https://doi.org/10.1063/1.4752434>.
- [29] L. Wang, S. Jenatsch, B. Ruhstaller, C. Hinderling, D. Gesevičius, R. Hany, F. Nüesch. *Adv. Func. Mater.* **2018**, *28*, 1705724, <https://doi.org/10.1002/adfm.201705724>.
- [30] G. C. Fish, J. M. Moreno-Naranjo, A. Billion, D. Kratzert, E. Hack, I. Krossing, F. Nüesch, J.-E. Moser. *Phys. Chem. Chem. Phys.* **2021**, *23*, 23886, <https://doi.org/10.1039/D1CP03251H>.
- [31] D. Amarasinghe Vithanage, A. Devižis, V. Abramavičius, Y. Infahsaeng, D. Abramavičius, R. C. I. MacKenzie, P. E. Keivanidis, A. Yartsev, D. Hertel, J. Nelson, V. Sundström, V. Gulbinas. *Nat. Commun.* **2013**, *4*, 2334, <https://doi.org/10.1038/ncomms3334>.

- [32] A. E. Jailaubekov, A. P. Willard, J. R. Tritsch, W.-L. Chan, N. Sai, R. Gearba, L. G. Kaake, K. J. Williams, K. Leung, P. J. Rossky, X.-Y. Zhu. *Nat. Mater.* **2013**, *12*, 66, <https://doi.org/10.1038/nmat3500>.
- [33] A. A. Bakulin, A. Rao, V. G. Pavelyev, P. H. M. van Loosdrecht, M. S. Pshenichnikov, D. Niedzialek, J. Cornil, D. Beljonne, R. H. Friend. *Science* **2014**, *335*, 6074.
- [34] G. Grancini, M. Maiuri, D. Fazzi, A. Petrozza, H.-J. Egelhaaf, D. Brida, G. Cerullo, G. Lanzani. *Nat. Mater.* **2013**, *12*, 29, <https://doi.org/10.1038/nmat3502>.
- [35] M. E. F. Bouduban, A. Burgos-Caminal, J. Teuscher, J.-E. Moser. *Chimia* **2017**, *71*, 231, <https://doi.org/10.2533/chimia.2017.231>.
- [36] M. Causa, J. De Jonghe-Risse, M. Scarongella, J. C. Brauer, E. Buchaca-Domingo, J.-E. Moser, N. Stingelin, N. Banerji. *Nat. Commun.* **2016**, *7*, 12556, <https://doi.org/10.1038/ncomms12556>.
- [37] A. A. Paraecattil, J. De Jonghe-Risse, V. Pranculis, J. Teuscher, J.-E. Moser. *J. Phys. Chem. C.* **2016**, *120*, 19595, <https://doi.org/10.1021/acs.jpcc.6b08022>.
- [38] A. Devišis, J. De Jonghe-Risse, R. Hany, F. Nüesch, S. Jenatsch, V. Gulbinas, J.-E. Moser. *J. Am. Chem. Soc.* **2015**, *137*, 8192, <https://doi.org/10.1021/jacs.5b03682>.

#### License and Terms



This is an Open Access article under the terms of the Creative Commons Attribution License CC BY 4.0. The material may not be used for commercial purposes.

The license is subject to the CHIMIA terms and conditions: (<https://chimia.ch/chimia/about>).

The definitive version of this article is the electronic one that can be found at <https://doi.org/10.2533/chimia.2022.552>